Rab13 regulates membrane trafficking between TGN and recycling endosomes in polarized epithelial cells

Rita L. Nokes,[1] Ian C. Fields,[1] Ruth N. Collins,[2] and Heike Fölsch[1]

[1]Department of Biochemistry, Molecular Biology and Cell Biology, Northwestern University, Evanston, IL 60208
[2]Department of Molecular Medicine, Veterinary Medical College, Cornell University, Ithaca, NY 14853

To maintain polarity, epithelial cells continuously sort transmembrane proteins to the apical or basolateral membrane domains during biosynthetic delivery or after internalization. During biosynthetic delivery, some cargo proteins move from the trans-Golgi network (TGN) into recycling endosomes (RE) before being delivered to the plasma membrane. However, proteins that regulate this transport step remained elusive. In this study, we show that Rab13 partially colocalizes with TGN38 at the TGN and transferrin receptors in RE. Knockdown of Rab13 with short hairpin RNA in human bronchial epithelial cells or overexpression of dominant-active or dominant-negative alleles of Rab13 in Madin-Darby canine kidney cells disrupts TGN38/46 localization at the TGN. Moreover, overexpression of Rab13 mutant alleles inhibits surface arrival of proteins that move through RE during biosynthetic delivery (vesicular stomatitis virus glycoprotein [VSVG], A-VSVG, and LDLR-CT27). Importantly, proteins using a direct route from the TGN to the plasma membrane are not affected. Thus, Rab13 appears to regulate membrane trafficking between TGN and RE.

Introduction

Polarized epithelial cells exhibit two functionally and biochemically distinct plasma membrane domains, which are separated by tight junctions (Nelson, 2003). To maintain this apical/basolateral polarity, cells must constantly sort transmembrane proteins to the correct locations during biosynthetic and endocytic delivery (Fölsch, 2008). Sorting of internalized cargo takes place in perinuclear recycling enzymes (RE), whereas sorting of newly synthesized cargo takes place at the TGN or in RE (see Fig. 2 A; Ang et al., 2004; Cancino et al., 2007). For example, a cargo thought to follow a direct pathway from the TGN to the apical membrane is influenza HA (hereafter referred to as HA; Fullekrug and Simons, 2004), and basolateral cargos thought to follow a direct pathway are FcII-B2 receptors (FcR) and a mutant low density lipoprotein receptor (LDLR[Y18A]; Simmen et al., 2002; Fields et al., 2007). These cargos are either segregated into glycolipid rafts (HA) or may interact with adaptor proteins that are recruited to the TGN such as AP-4 (LDLR[Y18A]; Simmen et al., 2002; Fullekrug and Simons, 2004; Fields et al., 2007). In contrast, cargos moving from the TGN into RE during biosynthetic delivery to the plasma membrane are vesicular stomatitis virus glycoprotein (VSVG), an apical variant of VSVG (A-VSVG), and a truncated version of LDLR (LDLR-CT27; Ang et al., 2004; Fields et al., 2007; Gravotta et al., 2007). At RE, cargos destined for the basolateral membrane frequently rely on the epithelial cell-specific adaptor complex AP-1B for sorting (Fölsch, 2005; Fields et al., 2007), whereas cargo destined for the apical membrane may segregate into Rab11-positive apical RE before being delivered to the apical membrane (Mostov et al., 2003; Thompson et al., 2007). Other transmembrane proteins such as the TGN resident protein TGN38 may travel through RE after internalization from the plasma membrane on their way back to the TGN (Ghosh et al., 1998). Despite our increasing knowledge of proteins that traffic between the TGN and RE, we know virtually nothing about the proteins regulating this step.

Correspondence to Heike Fölsch: h-folsch@northwestern.edu

Abbreviations used in this paper: CHX, cycloheximide; FcR, FcII-B2 receptor; GAPDH, glyceraldehyde 3-phosphate dehydrogenase; HBE, human bronchial epithelial; LDLR, low density lipoprotein receptor; mRFP, monomeric red fluorescent protein; RE, recycling endosomes; shRNA, short hairpin RNA; TfnR, transferrin receptor; VSVG, vesicular stomatitis virus glycoprotein.

The online version of this article contains supplemental material.

The Rockefeller University Press $30.00
J. Cell Biol. Vol. 182 No. 5 845–853
www.jcb.org/cgi/doi/10.1083/jcb.200802176

In general, membrane trafficking is regulated by small GTPases of the Ras superfamily. For example, in yeast, the Rab protein Sec4p regulates exocytic transport to the emerging bud (Novick and Guo, 2002). Among the closest mammalian homologues of Sec4p are Rab8, Rab10, and Rab13 (Pereira-Leal and Seabra, 2001; Collins, 2005; Buvelot Frei et al., 2006). In polarized epithelial cells, Rab8 plays a role in exocytosis of AP-1B–dependent cargo from the RE to the basolateral membrane (Ang et al., 2003). In addition, Rab8a activity is necessary for the outgrowth of the primary cilium (Nachury et al., 2007; Yoshimura et al., 2007). Likewise, Rab10 regulates endosomal sorting of internalized cargos (Babbey et al., 2006; Chen et al., 2006), and/or surface delivery of newly synthesized basolateral cargos (Schuck et al., 2007).

In contrast, Rab13 seems to regulate tight junction integrity. In MDCK cells stably expressing dominant-active Rab13Q67L but not dominant-negative Rab13T22N, mutants delayed tight junction formation (Marzesco et al., 2002). This effect might be caused by impaired endocytic recycling of the tight junction proteins claudin-1 and occludin, and down-regulation of PKA activity (Marzesco et al., 2002; Yamamoto et al., 2003; Kohler et al., 2004; Morimoto et al., 2005). However, these studies did not address whether Rab13 might also play a role during biosynthetic delivery of transmembrane proteins. Here, we show that Rab13 regulates surface delivery of cargos that travel through RE during biosynthetic delivery.

Results and discussion

To test whether Rab13 affects cell polarity, we microinjected V5-tagged Rab13Q67L or V5-tagged Rab13T22N cDNAs into filter-grown, fully polarized MDCK cells. Neither Rab13Q67L nor Rab13T22N overexpression disrupted basolateral localization of the marker protein gp58 (Fig. 1 A). Furthermore, tight junction assembly as judged by ZO-1 staining and cilium biogenesis were not affected (Fig. 1 B). Therefore, within the short times (4 h) of overexpression achieved by microinjection, the overall polarity is unaffected, in contrast to previous studies, which were based on prolonged overexpression (>24 h) of Rab13 mutants (Marzesco et al., 2002; Morimoto et al., 2005).

Using microinjection, we asked whether Rab13 mutants have any effects on surface delivery of VSVG. As a transmembrane protein, VSVG passes through the canonical biosynthetic pathway, from the ER and Golgi to the TGN. It then traverses the RE, from which it is sorted to the basolateral membrane in the AP-1B pathway (Fig. 2 A, 3 and 3b). Filter-grown MDCK cells were coinjected with cDNAs encoding Rab13 mutants and a CFP-tagged, temperature-sensitive mutant of VSVG (VSVG-CFPts045; Toomre et al., 1999). Cells were incubated for 2 h at the nonpermissive temperature of 39°C, at which VSVG accumulated in the ER, whereas Rab13 mutants were produced in the cytosol. To release VSVG from the ER for surface delivery, cells were shifted to 31°C for 2 h in the presence of cycloheximide (CHX) to prevent further protein synthesis. VSVG localized at the plasma membrane was detected with antibodies recognizing its ectodomain before fixation. Cells were then fixed, permeabilized, and stained for Rab13 and total VSVG. Although VSVG arrived at the basolateral surface in control cells, coinjection of either mutant allele severely blocked surface delivery (Fig. 1 C). We noted that the signal intensity of total VSVG also decreased, which perhaps indicates a missorting into lysosomes. Therefore, we incubated the cells with lysosomal inhibitors (50 μM ammonium chloride) and proteasomal inhibitors (3 mM MG132) to inhibit protein degradation during the chase. This treatment enhanced the signal for VSVG without restoring surface delivery (Fig. S1 A, available at http://www.jcb.org/cgi/content/full/jcb.200802176/DC1). Overall, we observed impaired surface delivery in 98% of cells analyzed expressing Rab13Q67L and in 97% of cells expressing Rab13T22N (Fig. S1 C).

To test whether Rab13 functions before or after VSVG moves into the Golgi, coverslip-grown MDCK cells were coinjected with cDNAs encoding VSVG-CFPts045 and V5-Rab13 mutants. Cells were incubated at 39°C for 2 h followed by 2 h at 20°C in the presence of CHX. During the 20°C incubation, VSVG exited the ER and became trapped in the Golgi. Specimens were fixed and immunolabeled for the cis-Golgi marker GM130, GFP, and V5-Rab13. There was no discernible difference in the transport of VSVG into the Golgi as judged by colocalization of VSVG and GM130 in control cells and those coinjected with Rab13 mutants (Fig. 1 D). Colocalization was observed in virtually 100% of cells analyzed independent of Rab13 overexpression. Thus, Rab13 may function in surface delivery of proteins downstream of the Golgi.

To narrow down which post-Golgi trafficking steps might be regulated by Rab13, we tested the effect of Rab13 overexpression by microinjection on the surface delivery of other reporter proteins. First, we analyzed LDLR-CT27, which is sorted to the basolateral membrane similar to VSVG (Fig. 2 A, 3 and 3b; Fields et al., 2007). We found that surface delivery of LDLR-CT27 was severely inhibited by both Rab13Q67L (93% of cells analyzed) and Rab13T22N (90% of cells analyzed) overexpression (Figs. 2 B and S1 C). Next, we tested LDLR(Y18A) and FcR, receptors that are thought to travel directly from the TGN to the basolateral surface independent of AP-1B function (Fig. 2 A, 1; Roush et al., 1998; Fields et al., 2007). Overexpression of Rab13 mutants had no effect on surface delivery of LDLR(Y18A) or FcR (Fig. 2, C and D).

Finally, we tested influenza HA and an apical mutant of VSVG (A-VSVG). Although the HA protein is sorted directly from the TGN to the apical membrane (Fig. 2 A, 2; Schuck and Simons, 2004), A-VSVG moves through RE (Fig. 2 A, 3 and 3a; Ang et al., 2004). We found no inhibition of surface delivery for HA in the presence of overexpressed Rab13 mutants (Fig. 2 E). In contrast, overexpression of Rab13Q67L or Rab13T22N severely inhibited surface delivery of A-VSVG (Fig. 2 F). Again, we found decreased fluorescent signals of A-VSVG in the cells. However, as was the case for VSVG, inhibition of protein degradation with ammonium chloride (50 μM) and MG132 (3 mM) raised the signal intensity without rescuing surface delivery (Fig. S1 B). The lack of surface arrival for A-VSVG was observed in 100% of cells analyzed expressing Rab13Q67L and in 100% of cells analyzed expressing Rab13T22N (Fig. S1 C).

Collectively, we found that cargos that travel to the surface via RE (LDLR-CT27, VSVG, and A-VSVG) were stalled within

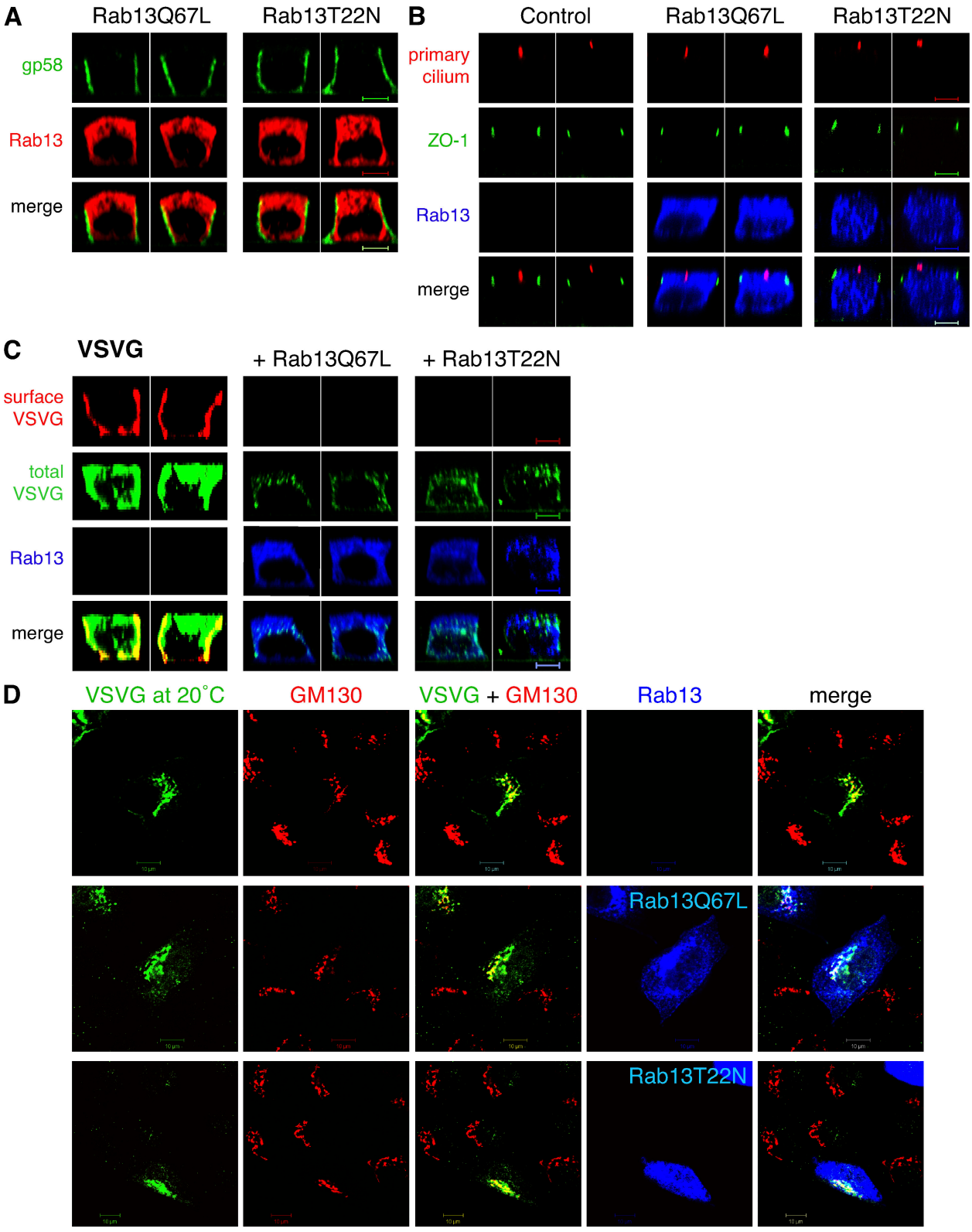

Figure 1. **Overexpression of Rab13 mutants affects surface delivery of VSVG.** (A–C) Filter-grown MDCK cells were microinjected with cDNAs encoding V5-Rab13Q67L or V5-Rab13T22N alone or together with cDNAs encoding VSVG-CFPts045 (see text for details). (A) Cells were costained for Rab13 and gp58. (B) Cells were triple-labeled for Rab13, primary cilia, and ZO-1. (C) Cells were labeled for surface VSVG, total VSVG, and Rab13. (D) MDCK cells seeded on coverslips were coinjected with cDNAs encoding VSVG-CFPts045 alone or together with cDNAs encoding V5-Rab13Q67L or V5-Rab12T22N (see text for details). Cells were immunolabeled for VSVG, Rab13, and GM130. For quantification, cells were scored for colocalization between VSVG and GM130. Data (see text) are mean values from at least three independent experiments (at least 30 cells per condition). Bars: (A–C) 5 μm; (D) 10 μm.

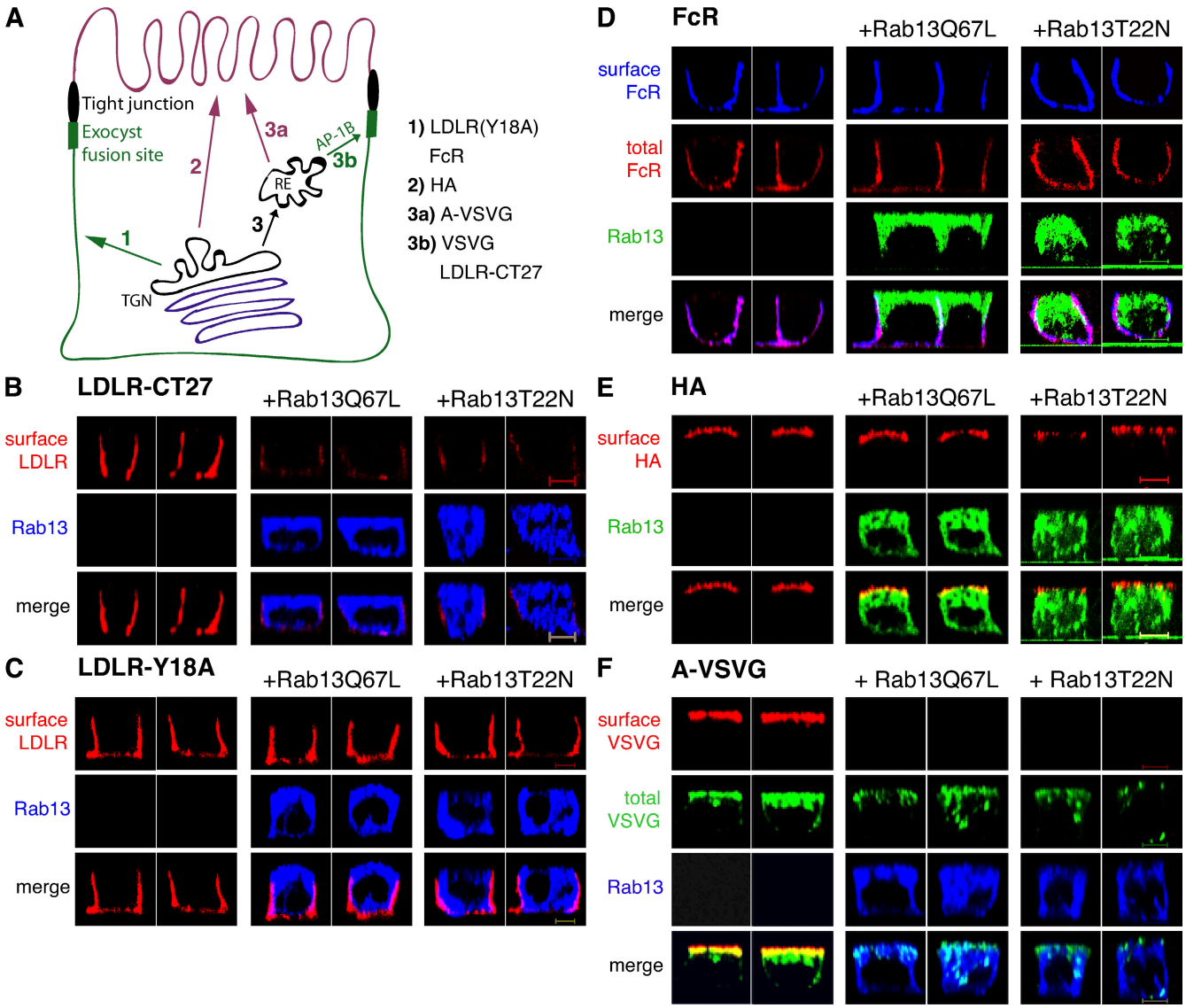

Figure 2. **Rab13 overexpression affects selective cargos.** (A) The model depicts trafficking pathways between the TGN and plasma membrane domains (see text for details). (B–F) Fully polarized MDCK cells were coinjected with cDNAs encoding V5-Rab13Q67L or V5-Rab13T22N and cDNAs encoding various reporter proteins. (B and C) cDNAs encoding V5-Rab13 mutants were coinjected with cDNAs encoding either LDLR-CT27 (B) or LDLR(Y18A) (C). Cells were incubated for 1 h at 37°C followed by 4 h at 20°C and 2 h at 37°C with CHX, and then stained for Rab13 and surface LDLR. (D) For expression of FcR, cDNAs encoding mRFP-tagged FcR were coinjected with cDNAs encoding Rab13 mutants. Cells were incubated for 1 h at 37°C and 2 h at 20°C followed by 2 h at 37°C with CHX, and then stained for Rab13 and surface FcR. (E) Cells microinjected to express Rab13 mutants together with HA were incubated for 1 h at 37°C followed by 4 h at 20°C and 2 h at 37°C with CHX, and then stained for Rab13 and surface HA. (F) cDNAs expressing Rab13 mutants or A-VSVG-GFPts045 were coinjected, and cells were processed as described for VSVG. Bars, 5 µm.

the cells upon overexpression of Rab13 mutants. In contrast, cargos not traversing the RE, such as the basolateral cargos LDLR(Y18A) and FcR as well as the apical cargo HA, were not affected. Because both VSVG and its apical variant A-VSVG were affected, Rab13 appears to function between the TGN and RE, as opposed to regulating post-RE trafficking pathways, which are different for VSVG and A-VSVG.

Because Rab13 appears to function at the TGN or RE, we sought to determine its detailed intracellular location. To this end, we used defective adenoviruses to express low levels of wild-type, GFP-tagged Rab13 (GFP-Rab13) in MDCK cells grown on coverslips. Coinfection with defective adenoviruses encoding GFP-Rab13 and µ1A-HA or µ1B-myc was used to monitor Rab13's localization relative to AP-1A or AP-1B, respectively. Rab13 colocalized with AP-1A at the TGN in 97 ± 7% of cells analyzed (Fig. 3 A). Note that although Rab13 did not colocalize entirely with AP-1A, almost all AP-1A staining colocalized with Rab13. In addition, Rab13 partially colocalized with AP-1B in RE in 76 ± 15% of cells analyzed (Fig. 3 B). We then analyzed Rab13 staining versus TGN38 (a marker for AP-1A–positive TGN) and transferrin receptor (TfnR; a marker for AP-1B–positive RE) in the same cells (Fölsch et al., 2003). Again, Rab13 partially colocalized with both TGN38 (98 ± 3% of cells analyzed) and TfnR (95 ± 8% of cells analyzed; Fig. 3 C). Furthermore, we found no colocalization between Rab13 and GM130 (not depicted). In addition to TGN/RE localization,

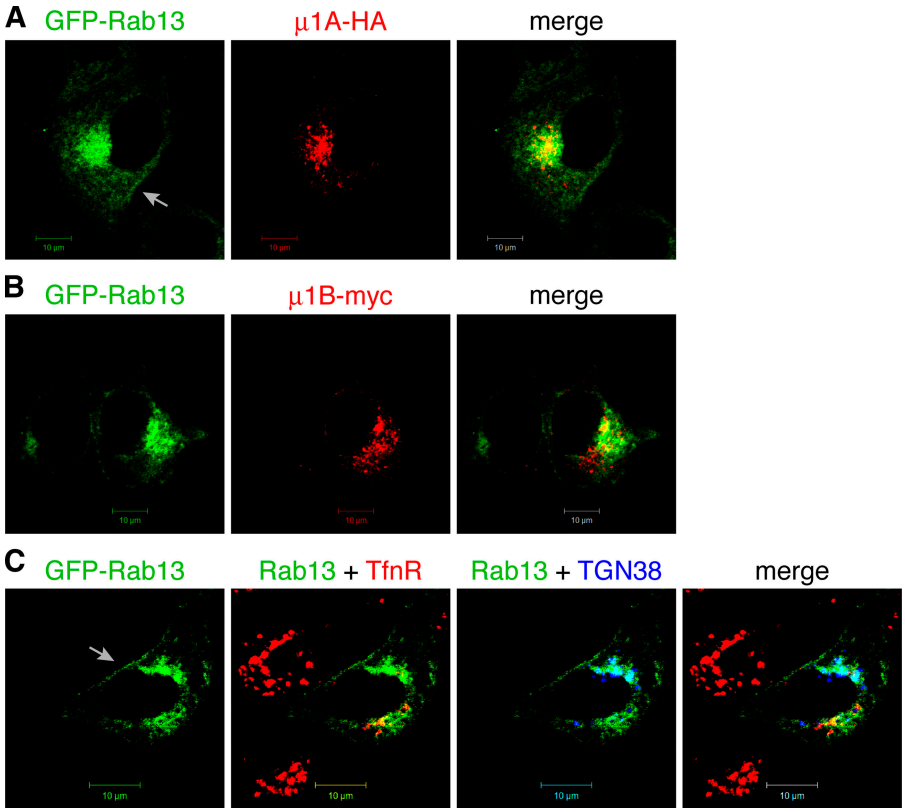

Figure 3. **Intracellular localization of Rab13.** MDCK cells grown on coverslips were infected with defective adenoviruses encoding GFP-V5-Rab13 wild type together with defective adenoviruses encoding μ1A-HA (A), μ1B-myc (B), or TGN38 (C). 24 h (C) or 36 h (A and B) after infection, cells were fixed and stained for HA, myc, TfnR, or TGN38. Arrows (A and C) indicate plasma membrane localization of Rab13. For quantification, cells were scored for at least partial overlapping staining. Data (see text) are mean values from at least four independent experiments (μ1A-HA, 30 cells; μ1B-myc, 65 cells; TfnR, 65 cells; TGN38, 61 cells), and errors indicate SD. Bars, 10 μm.

some Rab13 stained the plasma membrane (Fig. 3, A and C, arrows; Marzesco et al., 2002). Because Rab proteins localize to both donor and acceptor membranes (Collins, 2003), the partial localization of Rab13 at the TGN and RE supports our hypothesis that Rab13 functions at the interface between TGN and RE in addition to its described function at the tight junctions (Marzesco et al., 2002).

Next, we tested whether overexpression of Rab13 mutants might affect the TGN. We coinjected Rab13Q67L or Rab13T22N cDNAs together with TGN38 cDNAs into MDCK cells grown on coverslips. TGN38 is localized at the TGN in cells coinjected with an unrelated plasmid (mRFP-FcR cDNA; Fig. 4 A), whereas coexpression of Rab13Q67L or Rab13T22N dispersed TGN38 localization (Fig. 4 B and not depicted). This phenotype was observed in 97% of cells analyzed for Rab13Q67L and ∼80% of the cells analyzed for Rab13T22N (Fig. 4 E). In addition, TGN38 might be misrouted into lysosomes because staining intensities also decreased. This effect was specific because overexpression of Rab13 mutants by microinjection had no discernible effect on the localization of GM130, γ-adaptin (AP-1A and AP-1B), TfnR, or AP-3 (Fig. S2, available at http://www.jcb.org/cgi/content/full/jcb.200802176/DC1, and not depicted). Interestingly, the TGN marker protein furin was also not affected upon overexpression of Rab13 mutants by microinjection (Fig. S2 D), which indicates that perhaps only a subdomain of the TGN is affected by Rab13 or that only the retrieval pathway of TGN38, but not the retrieval pathway of furin, is inhibited by Rab13 overexpression.

Prolonged overexpression of Rab13 for 24 h by transient transfection disrupted the entire Golgi, as judged by a more dispersed GM130 staining, whereas γ-adaptin and TfnR remained fine (Fig. S3, available at http://www.jcb.org/cgi/content/full/jcb.200802176/DC1). Notably, cells transiently overexpressing Rab13Q67L for prolonged times may compensate by expressing more GM130, as judged by its more intense GM130 staining (Fig. S3 A). Although this phenotype prevented us from using defective adenoviruses for biochemical analysis, this finding might reconcile our data with the published literature. Over time, disruption of the Golgi may lead to polarity defects. In addition, overexpression of Rab13Q67L may lead to tight junction defects perhaps caused by enhanced delivery of activated Rab13 to the tight junctions. Importantly, our study is the first one to demonstrate any phenotype for the Rab13T22N allele. Therefore, it seems likely that Rab13's primary function may be in controlling membrane trafficking between TGN and RE.

To confirm Rab13's effects on the TGN by an independent assay, we knocked down Rab13 in human bronchial epithelial (HBE) cells (the 16HBE14o$^-$ strain was used). Like MDCK cells, this cell line expresses Rab13 and μ1B based on RT-PCR, and fully polarized HBE cells sort LDLR-CT27 to the basolateral membrane and grow out a single primary cilium (unpublished data). In addition, HBE cells form ZO-1 containing tight junctions (Kizhatil et al., 2007). We obtained three GFP-tagged short hairpin RNA (shRNA) constructs targeting Rab13 and one control construct targeting glyceraldehyde 3-phosphate dehydrogenase (GAPDH) from Thermo Fisher Scientific. To test knockdown capacities, shRNA constructs were transfected into HBE cells together with a dual expression plasmid encoding both monomeric red fluorescent protein (mRFP) and T7-tagged Rab13 from different promoters. 48 h after

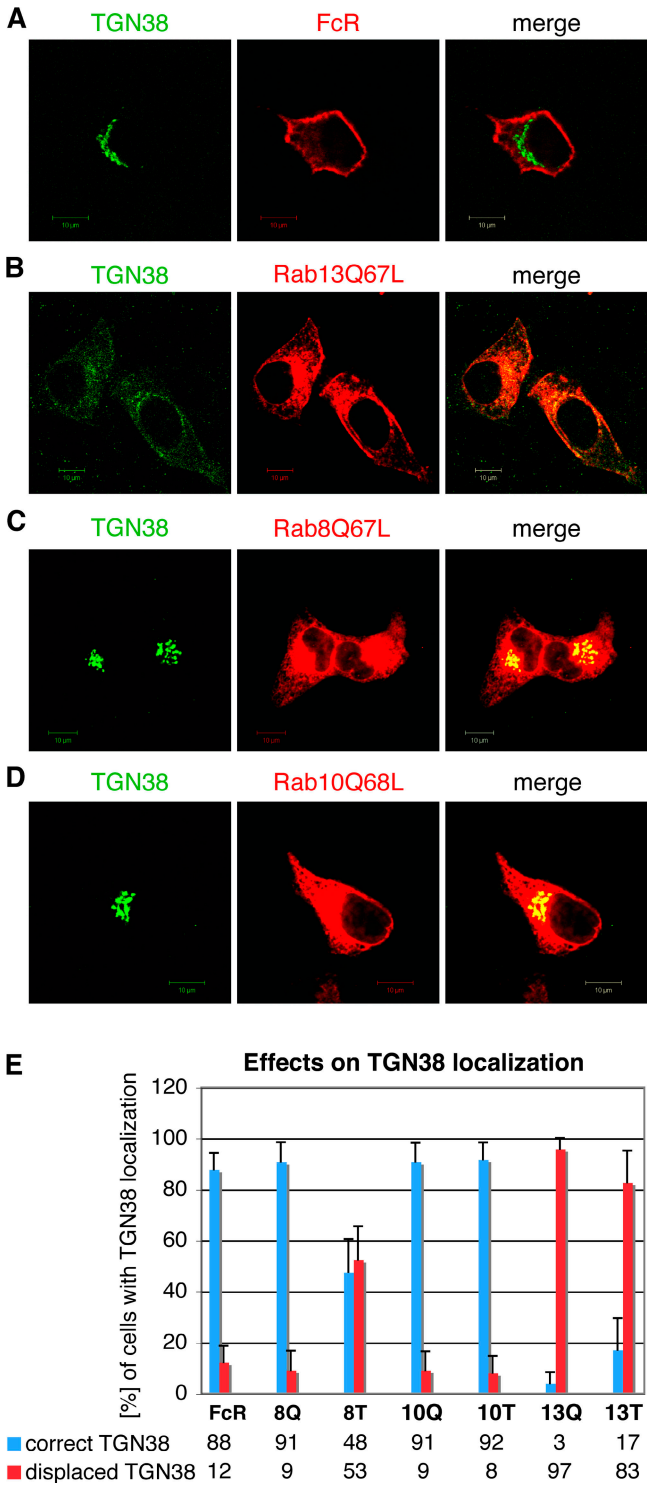

Figure 4. **Overexpression of Rab13 mutants disrupts TGN38.** (A–D) MDCK cells grown on coverslips were microinjected with cDNAs encoding TGN38 or mRFP-FcR (A), or TGN38 together with cDNAs encoding V5-Rab13Q67L (B), T7-Rab8Q67L (C), or T7-Rab10Q68L (D). Cells were incubated at 39 and 31°C as described for VSVG. Cells were stained for TGN38 and Rab proteins. Bars, 10 µm. (E) Cells coinjected with TGN38 and Rab cDNAs were scored for correct or displaced TGN38 localization. Data are mean values from at least three independent experiments totaling 70 to 80 cells for each condition. Error bars indicate SD. Q, Q67L allele; T, T22N allele of the indicated Rab.

transfection, cells were immunolabeled for Rab13 and analyzed by confocal microscopy (Fig. 5 A). We then calculated values for Rab13 knockdown as described in Materials and methods. Constructs Rab13 Nos. 1 and 3 decreased Rab13 expression by 87 and 82% (Fig. 5 A), respectively, whereas construct No. 2 was not effective (not depicted). Next, we tested the effect of Rab13 knockdown on endogenous TGN46 and GM130. We observed a disruption and/or loss of TGN46 staining in ∼57% of cells analyzed for construct No. 1 and in ∼80% of cells analyzed for construct No. 3 (Fig. 5 B). These data indicate that Rab13 is indeed necessary for the maintenance of TGN38/46 localization at the TGN. Interestingly, as was the case with prolonged Rab13 overexpression, knockdown of Rab13 also led to a disruption/loss of GM130 staining in 43% of cells analyzed for construct No. 1 and 62% of cells analyzed for construct No. 3 (Fig. 5 B). Recently, it was shown that Rab13 knockdown in MDCK cells disrupted tight junctions (Yamamura et al., 2008). Therefore, it seems that prolonged overexpression and knockdown of Rab13 share the same phenotypes in disrupting TGN38/46 and GM130 localization at the TGN/Golgi together with impairing tight junctions. This is in contrast to acute overexpression by microinjection, which leaves the tight junctions and the Golgi mainly intact.

Previously, Rab8 and Rab10, close homologues of Rab13, were shown to result in apical missorting of VSVG upon overexpression of mutant Rab proteins (Ang et al., 2003; Schuck et al., 2007). Therefore, the inhibition of surface delivery is unique to Rab13. To test whether Rab13 may have an equally unique function in TGN38 localization, we injected cDNAs encoding Rab8 or Rab10 mutants together with plasmids encoding TGN38 into MDCK cells and analyzed TGN38 localization. Neither Rab8Q67L nor Rab10Q68L or Rab10T23N had any discernible effects on TGN38 localization in >90% of cells analyzed (Fig. 4, C–E; and not depicted). Interestingly, when Rab8T22N was coinjected with TGN38 cDNA, ∼50% of the cells lacked TGN38 staining (Fig. 4 E). Note, during biosynthetic delivery of AP-1B cargos, only Rab8Q67L, but not Rab8T22N, showed any effects on basolateral delivery from RE (Ang et al., 2003). However, because Rab8 localizes in RE (Ang et al., 2003), overexpression of Rab8T22N might interfere with retrieval pathways back to the TGN from early endosomes through RE. Regardless, the effects on TGN38 localization are most pronounced upon overexpression of both Rab13 mutants, indicating that Rab13's effects on TGN38 are specific for Rab13.

In summary, Rab13 clearly differs from its homologues Rab8 and Rab10 with respect to two key assays. First, overexpression of Rab13 mutants inhibited surface delivery in the biosynthetic pathway of both apical and basolateral cargos that move through RE as opposed to apical missorting of AP-1B–dependent cargos (Ang et al., 2003; Schuck et al., 2007). Therefore, Rab13 appears to operate at an earlier membrane trafficking step distinct from Rab8 or Rab10. Second, in contrast to Rab13Q67L, neither Rab8Q67L nor Rab10Q68L showed any effects on TGN38 localization at the TGN. Having established a role for Rab13 at the interface between TGN and RE, we can now begin to analyze Rab13's interplay with known regulators of the TGN.

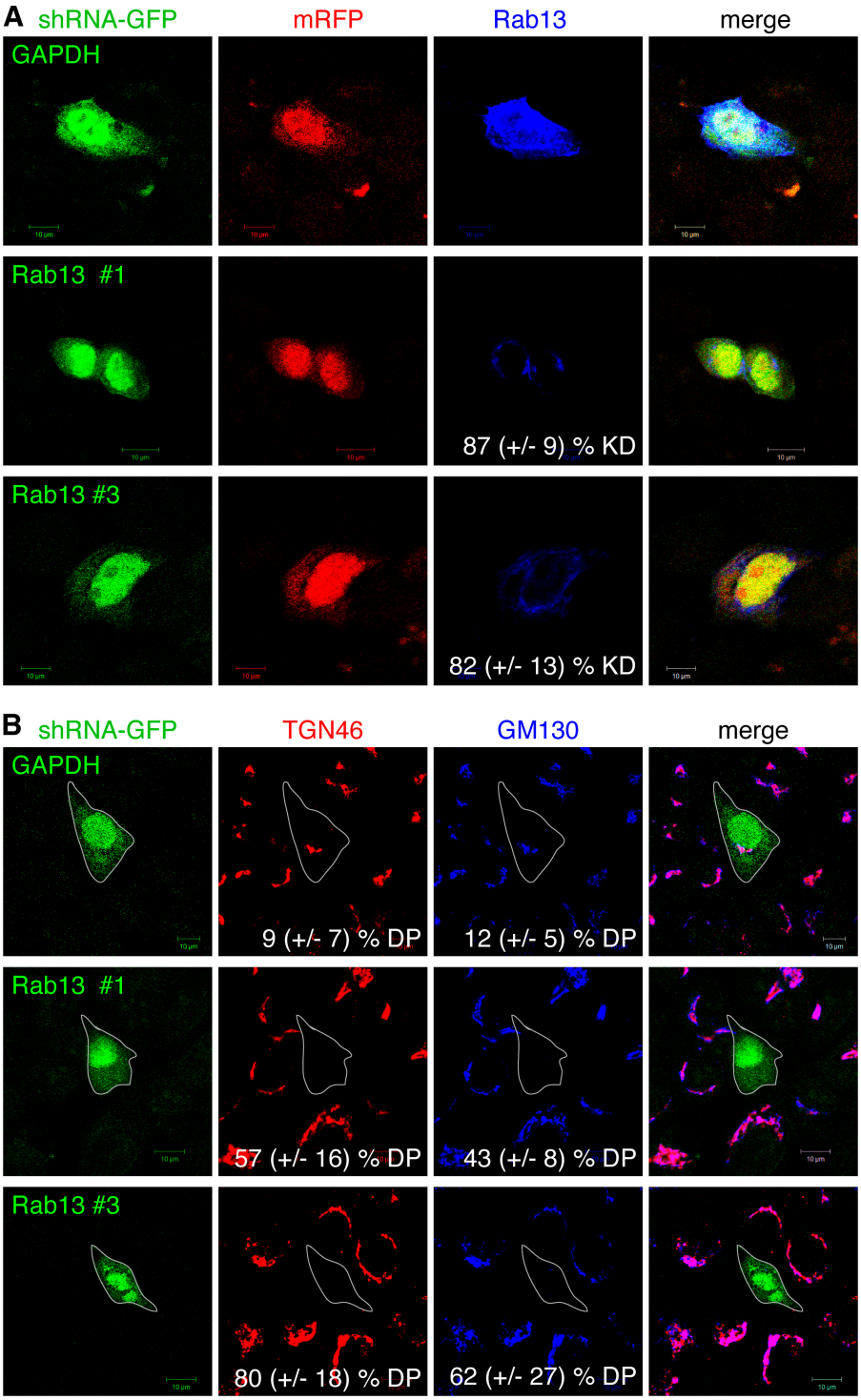

Figure 5. **Knockdown of Rab13 in HBE cells disrupts TGN46 and GM130.** (A) HBE cells grown on coated coverslips were cotransfected with plasmids encoding shRNA constructs and dual-expression plasmids encoding mRFP and T7-Rab13. 48 h after transfection, cells were fixed and stained for Rab13. Rab13 knockdown was calculated from three independent experiments, counting at least 30 cells (errors indicate SD). (B) Coverslip-grown HBE cells were transfected with plasmids encoding shRNA constructs. After 48 h, cells were fixed and stained for TGN46 and GM130. At least 50 cells from at least three independent experiments were scored for TGN46 or GM130 staining (errors indicate SD). Cells transfected with shRNAs are outlined in white. DP, disruption phenotype; KD, knockdown. Bars, 10 μm.

Materials and methods

Cloning, RNAi constructs, and adenoviruses

The open reading frame of human Rab13 was cloned by coupled RT-PCR using the gene-specific PCR primers 5′-ATATAAACATAACAAGATAAACATGGCCAAAGCCTACGAC-3′ and 5′-TCTTCTTTTCTTCAGCCCAGGGAGCACTTG-3′. Subsequently, Rab13 was used as a template to generate V5-tagged Rab13 using the N- and C-terminal primers 5′-GCAGATCTATGGGAAAGCCAATACCAAACCCCTTATTAGGATTAGACAGCACAGCCAAAGCCTACGACCACCTCTTC-3′ and 5′-GCGCAAGCTTTCAGCCCAGGGAGCACTTGTTGGT-3′, respectively. The PCR products were cloned as BglII–HindIII fragments into the microinjection vector pRKV or the adenovirus shuttle vector pShuttle-cytomegalovirus (CMV). EGFP-V5–tagged Rab13 was cloned by inserting DNA encoding EGFP into the BglII site of pShuttle-CMV as BglII–BamHI fragments. T22N and Q67L mutations were introduced into Rab13 by QuikChange site-directed mutagenesis (Stratagene) using V5-Rab13 in pRKV as a template and matching sense/antisense primer pairs. The sense primer for T22N was 5′-GGGTGGGCAAGAATTGTCTGATCAT-3′, and the sense primer for Q67L mutagenesis was 5′-ACACGGCTGGCCTAGAGCGGTTCAA-3′. T7-tagged Rab13 was generated using the N-terminal primer 5′-GCGCAGATCTATGGCTAGCATGACTGGTGGACAGCAAATGGGTGCCAAAGCCTACGACCACCTCTTC-3′ and the same C-terminal primers and template as before. T7-Rab13 PCR products were cloned as BglII–BamHI fragments behind the CMV promoter in

pBUDCE4. Subsequently, mRFP was cloned behind the EF-1α promoter of pBUDCE4 as KpnI–BamHI PCR fragments. mRFP was amplified using mRFP-FcR as a template and the N- and C-terminal primers 5′-GCGCGGTACCATGGCCTCCTCCGAGGACGTCATC-3′ and 5′-GCGCGGATCCTTAGGCGCCGGTGGAGTGGCGGCCCTC-3′, respectively.

Plasmids expressing canine Rab10 and mutant Rab10s were obtained from K. Simons (Max-Planck-Insititut for Molecular Cell Biology and Genetics, Dresden, Germany). We subsequently used these plasmids as templates to amplify T7-tagged Rab10 using the N- and C-terminal primers 5′-GCAGATCTATGGCTAGCATGACTGGTGGACAGCAAATGGGTGCGAAGAAGACGTACGACCTGCTTTTC-3′ and 5′-GCGCAAGCTTTCAGCAACATTTGCTCTTCCAGCC-3′, respectively. PCR products were cloned as BglII–HindIII fragments into pRKV.

T7-tagged Rab8 mutants in pRKV were as described previously (Ang et al., 2003). HA in vector pCAGGS was obtained from R. Lamb (Northwestern University, Evanston, IL). CFP-VSVG in pEYFP-N1 was obtained from D. Toomre (Yale University, New Haven, CN); GFP–A-VSVG in pRKV as well as TGN38, mRFP-FcR, LDLR-CT27, and LDLR(Y18A) in pShuttle-CMV were as described previously (Ang et al., 2003; Fields et al., 2007). Defective adenoviruses encoding μ1A-HA or μ1B-myc were as described previously (Fields et al., 2007). Defective adenoviruses encoding EGFP-V5-Rab13 or TGN38 were generated as described previously (Fölsch et al., 1999).

RNAi constructs targeting human Rab13 (oligo IDs V2LHS_171155, V2LHS_278139, and V2LHS_171156) or human GAPDH were obtained from Thermo Fisher Scientific. We obtained shRNAmir constructs in the lentiviral vector pGIPz, which expresses turboGFP-tagged shRNAs. The sequences were as follows: construct 1, 5′-TGCTGTTGACAGTGAGCGAGGATGAGAAATCTTTCGAGAATAGTGAAGCCACAGATGTATTCTCGAAAGATTTCTCATCCGTGCCTACTGCCTCGGA-3′ (V2LHS_171155); construct 2, 5′-TGCTGTTGACAGTGAGCGAGGTCACATAGGTAGATGGTAATAGTGAAGCCACAGATGTATTACCATCTACCTATGTGACCCTGCCTACTGCCTCGGA-3′ (V2LHS_278139); and construct 3, 5′-TGCTGTTGACAGTGAGCGACCTCCCAGTACTGACCTGAAATAGTGAAGCCACAGATGTATTTCAGGTCAGTACTGGGAGGCTGCCTACTGCCTCGGA-3′ (V2LHS_171156).

Cell culture

MDCK cells were cultured in MEM with the addition of 2 mM L-glutamine, 0.1 mg/ml penicillin/streptomycin, and 7% (vol/vol) fetal bovine serum at 37°C and 5% CO_2. HBE cells were obtained from D. Gruenert (California Pacific Medical Center, San Francisco, CA) and cultured on fibronectin-coated plates or coverslips in MEM with the addition of 2 mM L-glutamine, 0.1 mg/ml penicillin/streptomycin, and 10% (vol/vol) fetal bovine serum at 37°C and 5% CO_2. The coating solution contained LHC basal medium with 10 mg/100 ml bovine serum albumin, 3 mg/100ml bovine collagen I, and 1 mg/100ml fibronectin.

For microinjection experiments of polarized cells, 4×10^5 cells were seeded per 12-mm clear filter (0.4-μm pore size; Corning) and cultured for 3–4 d with changes of the medium in the basolateral chamber every day. After excision of the filter from the filter holders, cells were placed in 50 mM of Hepes-buffered media, and 0.2 mg/ml cDNAs were microinjected into the nuclei of the cells using a Femtojet microinjector (Injectman NI2; Eppendorf) mounted on an inverted microscope (Axiovert 200; Carl Zeiss, Inc.) with a heated stage.

For injection of ts045 mutants of VSVG and A-VSVG, cells were injected at 39°C; after injection, cells were incubated for 2 h at 39°C followed by 2 h at 31°C in the presence of 50 mM Hepes-buffered media and 0.1 mg/ml CHX with or without the addition of 0.05 mM MG132 and 3 mM ammonium chloride. Other cargos were injected at 37°C, followed by a 1-h incubation at 37°C and 2–4 h at 20°C in 50 mM Hepes-buffered media, which was followed by a chase at 37°C for 1–2 h in the presence of 0.1 mg/ml CHX. Subsequently, cells were processed for immunofluorescence microscopy (see "Immunofluorescence microscopy").

For immunofluorescence experiments with cells grown on coverslips, cells were seeded on Alcian blue or fibronectin/collagen-coated coverslips and cultured for 2–4 d. Infection of cells with defective adenoviruses was performed as described previously (Fields et al., 2007). Transient transfections were done using Lipofectamine 2000 (Invitrogen) according to the manufacturer's instructions.

Antibodies

Mouse monoclonal antibodies recognizing GM130 (610822) or TGN38 (T69020) were obtained from BD Biosciences. Mouse monoclonal antibodies recognizing acetylated tubulin (6-11B-1) or γ-adaptin (100/3) were obtained from Sigma-Aldrich. Mouse monoclonal antibodies recognizing ZO-1 (33–9100) were obtained from Invitrogen. Monoclonal antibodies against the T7 epitope (69522–3) were obtained from EMD, antibodies against the HA-epitope (16B12) were obtained from Covance, and antibodies recognizing the V5-epitope (336) were generated by R. Randall (University of St. Andrews, St. Andrews, Fife, Scotland, UK) and obtained from R. Lamb.

Rabbit polyclonal antibodies against furin (PA1-062) were obtained from Affinity BioReagents, anti-GFP antibodies (ab90) and anti-TGN46 antibodies (50595) were obtained from Abcam, and anti-myc antibodies (A-14) were obtained from Santa Cruz Biotechnology, Inc. Polyclonal antibodies against GM130 or TGN38 were a gift from G. Warren (Max F. Perutz Laboratories, Vienna, Austria). Goat polyclonal antibodies recognizing the ectodomain of HA (anti-H3 [A/HongKong/1/68], No. V-314-591-157) are available from the National Institute of Allergy and Infectious Diseases, National Institutes of Health.

Hybridomas producing antibodies against δ-adaptin (SA4) were generated by A. Peden (University of Cambridge, Cambridge, England, UK) and obtained from the Developmental Studies Hybridoma Bank. Hybridomas producing antibodies recognizing gp58, FcR (2.4G2), LDLR (C7), human TfnR (H68.4), or VSVG (TK1) were generated as described previously (Fields et al., 2007).

Secondary antibodies labeled with Alexa dyes were obtained from Invitrogen. Cy5-labeled antibodies were obtained from Jackson ImmunoResearch Laboratories, and Cy5-labeled goat anti–mouse IgG2a antibodies were obtained from SouthernBiotech.

Immunofluorescence microscopy

In general, cells were fixed in 3% PFA for 15 min at RT followed by an incubation in PBS^{2+} (PBS [0.2 g/liter KCl, 0.2 g/liter KH_2PO_4, 8 g/liter NaCl, and 2.17 g/liter $Na_2HPO_4 \times 7\ H_2O$] plus 0.1 g/liter $CaCl_2$ and 0.1 g/liter $MgCl_2 \times 6\ H_2O$) for 5 min. Subsequently, cells were incubated for 1 h in a blocking/permeabilization solution (BPS; 2% [wt/vol] BSA and 0.4% [wt/vol] saponin in PBS^{2+}) with 10% [vol/vol] goat serum. Cells were then incubated for 1 h with primary antibodies in BPS, followed by 5 washes over 30 min with BPS. Finally, cells were incubated for 1 h with secondary antibodies (often isotype specific) in BPS, followed by five washes in BPS. Cells were mounted in a solution containing 10% [wt/vol] DABCO and 50% [wt/vol] glycerol. For cell surface staining, cells were incubated with primary antibodies for 1 h on ice followed by washes with ice-cold PBS^{2+} before fixation.

Specimens were analyzed at room temperature using a confocal microscope (Microsystem LSM 510 with ConfoCor3 software) equipped with a 63× water immersion lens (all from Carl Zeiss, Inc.). Images were combined and enhanced using Photoshop (Adobe).

For quantification of shRNA knockdown, HBE cells were cotransfected with shRNA constructs and pBUDCE4 encoding mRFP and T7-Rab13 24 h after seeding. 48 h after transfection, cells were fixed, permeabilized, and stained for T7-Rab13. Images of specimens were taken under the same confocal settings, and mean pixel intensities were obtained using 510 ConfoCor 3 software (Carl Zeiss, Inc.). We then determined the ratio between T7-Rab13 and mRFP signals. The mean ratio of cells coexpressing a control shRNA construct targeting GAPDH was set 100%, and the values of knockdown for the Rab13 shRNA constructs were determined as percentage values of the control.

Online supplemental material

Fig. S1 shows the surface delivery of VSVG or A-VSVG in polarized MDCK cells treated with proteolysis inhibitors and quantification of surface delivery phenotypes for VSVG, A-VSVG, and LDLR-CT27. Fig. S2 shows that GM130, γ-adaptin, TfnR, and furin are not disrupted by overexpression of Rab13Q67L by microinjection. Fig. S3 shows the dispersal of GM130 upon transient overexpression of Rab13Q67L or Rab13T22N, whereas γ-adaptin and TfnR staining remained unaltered by this treatment. Online supplemental material is available at http://www.jcb.org/cgi/content/full/jcb.200802176/DC1.

We thank Drs. Derek Toomre, Graham Warren, Kai Simons, and Robert Lamb for reagents; and the Lamb laboratory for helpful discussions. We thank Dr. Bettina Winckler (University of Virginia) for comments on the manuscript. We thank Elina Shteyn and William Buggele for expert technical assistance.

This work was funded by a grant from the National Institutes of Health (GM070736) to H. Fölsch, and supported in part by a grant from the American Cancer Society (ACS-IRG #93-037-09) to H. Fölsch and a Katten Muchin Rosenman Travel Scholarship Award from the Robert H. Lurie Comprehensive Cancer Center of Northwestern University to R.L. Nokes. Work in the laboratory of R.N. Collins was supported by a grant from the National Institutes of Health (GM069596).

Submitted: 27 February 2008
Accepted: 4 August 2008

References

Ang, A.L., H. Fölsch, U.M. Koivisto, M. Pypaert, and I. Mellman. 2003. The Rab8 GTPase selectively regulates AP-1B–dependent basolateral transport in polarized Madin-Darby canine kidney cells. *J. Cell Biol.* 163:339–350.

Ang, A.L., T. Taguchi, S. Francis, H. Fölsch, L.J. Murrells, M. Pypaert, G. Warren, and I. Mellman. 2004. Recycling endosomes can serve as intermediates during transport from the Golgi to the plasma membrane of MDCK cells. *J. Cell Biol.* 167:531–543.

Babbey, C.M., N. Ahktar, E. Wang, C.C. Chen, B.D. Grant, and K.W. Dunn. 2006. Rab10 regulates membrane transport through early endosomes of polarized Madin-Darby canine kidney cells. *Mol. Biol. Cell.* 17:3156–3175.

Buvelot Frei, S., P.B. Rahl, M. Nussbaum, B.J. Briggs, M. Calero, S. Janeczko, A.D. Regan, C.Z. Chen, Y. Barral, G.R. Whittaker, and R.N. Collins. 2006. Bioinformatic and comparative localization of Rab proteins reveals functional insights into the uncharacterized GTPases Ypt10p and Ypt11p. *Mol. Cell. Biol.* 26:7299–7317.

Cancino, J., C. Torrealba, A. Soza, M.I. Yuseff, D. Gravotta, P. Henklein, E. Rodriguez-Boulan, and A. Gonzalez. 2007. Antibody to AP1B adaptor blocks biosynthetic and recycling routes of basolateral proteins at recycling endosomes. *Mol. Biol. Cell.* 18:4872–4884.

Chen, C.C., P.J. Schweinsberg, S. Vashist, D.P. Mareiniss, E.J. Lambie, and B.D. Grant. 2006. RAB-10 is required for endocytic recycling in the *Caenorhabditis elegans* intestine. *Mol. Biol. Cell.* 17:1286–1297.

Collins, R.N. 2003. "Getting it on"–GDI displacement and small GTPase membrane recruitment. *Mol. Cell.* 12:1064–1066.

Collins, R.N. 2005. Application of phylogenetic algorithms to assess Rab functional relationships. *Methods Enzymol.* 403:19–28.

Fields, I.C., E. Shteyn, M. Pypaert, V. Proux-Gillardeaux, R.S. Kang, T. Galli, and H. Fölsch. 2007. v-SNARE cellubrevin is required for basolateral sorting of AP-1B-dependent cargo in polarized epithelial cells. *J. Cell Biol.* 177:477–488.

Fölsch, H. 2005. The building blocks for basolateral vesicles in polarized epithelial cells. *Trends Cell Biol.* 15:222–228.

Fölsch, H. 2008. Regulation of membrane trafficking in polarized epithelial cells. *Curr. Opin. Cell Biol.* 20:208–213.

Fölsch, H., H. Ohno, J.S. Bonifacino, and I. Mellman. 1999. A novel clathrin adaptor complex mediates basolateral targeting in polarized epithelial cells. *Cell.* 99:189–198.

Fölsch, H., M. Pypaert, S. Maday, L. Pelletier, and I. Mellman. 2003. The AP-1A and AP-1B clathrin adaptor complexes define biochemically and functionally distinct membrane domains. *J. Cell Biol.* 163:351–362.

Fullekrug, J., and K. Simons. 2004. Lipid rafts and apical membrane traffic. *Ann. N. Y. Acad. Sci.* 1014:164–169.

Ghosh, R.N., W.G. Mallet, T.T. Soe, T.E. McGraw, and F.R. Maxfield. 1998. An endocytosed TGN38 chimeric protein is delivered to the TGN after trafficking through the endocytic recycling compartment in CHO cells. *J. Cell Biol.* 142:923–936.

Gravotta, D., A. Deora, E. Perret, C. Oyanadel, A. Soza, R. Schreiner, A. Gonzalez, and E. Rodriguez-Boulan. 2007. AP1B sorts basolateral proteins in recycling and biosynthetic routes of MDCK cells. *Proc. Natl. Acad. Sci. USA.* 104:1564–1569.

Kizhatil, K., W. Yoon, P.J. Mohler, L.H. Davis, J.A. Hoffman, and V. Bennett. 2007. Ankyrin-G and beta2-spectrin collaborate in biogenesis of lateral membrane of human bronchial epithelial cells. *J. Biol. Chem.* 282:2029–2037.

Kohler, K., D. Louvard, and A. Zahraoui. 2004. Rab13 regulates PKA signaling during tight junction assembly. *J. Cell Biol.* 165:175–180.

Marzesco, A.M., I. Dunia, R. Pandjaitan, M. Recouvreur, D. Dauzonne, E.L. Benedetti, D. Louvard, and A. Zahraoui. 2002. The small GTPase Rab13 regulates assembly of functional tight junctions in epithelial cells. *Mol. Biol. Cell.* 13:1819–1831.

Morimoto, S., N. Nishimura, T. Terai, S. Manabe, Y. Yamamoto, W. Shinahara, H. Miyake, S. Tashiro, M. Shimada, and T. Sasaki. 2005. Rab13 mediates the continuous endocytic recycling of occludin to the cell surface. *J. Biol. Chem.* 280:2220–2228.

Mostov, K., T. Su, and M. ter Beest. 2003. Polarized epithelial membrane traffic: conservation and plasticity. *Nat. Cell Biol.* 5:287–293.

Nachury, M.V., A.V. Loktev, Q. Zhang, C.J. Westlake, J. Peranen, A. Merdes, D.C. Slusarski, R.H. Scheller, J.F. Bazan, V.C. Sheffield, and P.K. Jackson. 2007. A core complex of BBS proteins cooperates with the GTPase Rab8 to promote ciliary membrane biogenesis. *Cell.* 129:1201–1213.

Nelson, W.J. 2003. Adaptation of core mechanisms to generate cell polarity. *Nature.* 422:766–774.

Novick, P., and W. Guo. 2002. Ras family therapy: Rab, Rho and Ral talk to the exocyst. *Trends Cell Biol.* 12:247–249.

Pereira-Leal, J.B., and M.C. Seabra. 2001. Evolution of the Rab family of small GTP-binding proteins. *J. Mol. Biol.* 313:889–901.

Roush, D.L., C.J. Gottardi, H.Y. Naim, M.G. Roth, and M.J. Caplan. 1998. Tyrosine-based membrane protein sorting signals are differentially interpreted by polarized Madin-Darby canine kidney and LLC-PK1 epithelial cells. *J. Biol. Chem.* 273:26862–26869.

Schuck, S., and K. Simons. 2004. Polarized sorting in epithelial cells: raft clustering and the biogenesis of the apical membrane. *J. Cell Sci.* 117:5955–5964.

Schuck, S., M.J. Gerl, A. Ang, A. Manninen, P. Keller, I. Mellman, and K. Simons. 2007. Rab10 is involved in basolateral transport in polarized Madin-Darby canine kidney cells. *Traffic.* 8:47–60.

Simmen, T., S. Honing, A. Icking, R. Tikkanen, and W. Hunziker. 2002. AP-4 binds basolateral signals and participates in basolateral sorting in epithelial MDCK cells. *Nat. Cell Biol.* 4:154–159.

Thompson, A., R. Nessler, D. Wisco, E. Anderson, B. Winckler, and D. Sheff. 2007. Recycling endosomes of polarized epithelial cells actively sort apical and basolateral cargos into separate subdomains. *Mol. Biol. Cell.* 18:2687–2697.

Toomre, D., P. Keller, J. White, J.C. Olivo, and K. Simons. 1999. Dual-color visualization of trans-Golgi network to plasma membrane traffic along microtubules in living cells. *J. Cell Sci.* 112:21–33.

Yamamoto, Y., N. Nishimura, S. Morimoto, H. Kitamura, S. Manabe, H.O. Kanayama, S. Kagawa, and T. Sasaki. 2003. Distinct roles of Rab3B and Rab13 in the polarized transport of apical, basolateral, and tight junctional membrane proteins to the plasma membrane. *Biochem. Biophys. Res. Commun.* 308:270–275.

Yamamura, R., N. Nishimura, H. Nakatsuji, S. Arase, and T. Sasaki. 2008. The interaction of JRAB/MICAL-L2 with Rab8 and Rab13 coordinates the assembly of tight junctions and adherens junctions. *Mol. Biol. Cell.* 19:971–983.

Yoshimura, S., J. Egerer, E. Fuchs, A.K. Haas, and F.A. Barr. 2007. Functional dissection of Rab GTPases involved in primary cilium formation. *J. Cell Biol.* 178:363–369.